Int. J. Solids Structures Vol. 30, No. 11, pp. 1491–1501, 1993
Printed in Great Britain

0020-7683/93 $6.00+ .00

CALCULATION OF STRESSES AT SKIN–STIFFENER INTERFACES OF COMPOSITE STIFFENED PANELS UNDER SHEAR LOADS

CHRISTOS KASSAPOGLOU
Structures Research Section, Sikorsky Aircraft Division (UTC), 6900 Main Street, Stratford, CT 06601, U.S.A.

(*Received* 12 *March* 1992; *in revised form* 16 *August* 1992)

Abstract—A simple energy-based approach to calculate stresses at skin–stiffener interfaces of composite stiffened panels under shear loads is presented. Solutions to the governing partial differential equations are sought that satisfy boundary conditions and traction continuity. The stress functional forms are determined by minimizing the energy using a variational approach. The resulting closed form stress expressions are compared to finite element solutions and are shown to be in very good agreement.

INTRODUCTION

The increased use of composite materials in primary aircraft structures has introduced failure modes that are not frequently encountered in equivalent metal structures. One of these failure modes is the separation of stiffeners from skins under generalized loading. A stiffened panel under load is shown in Fig. 1. Of particular interest is the case of stiffened skins under shear loadings. High peeling and interlaminar shear loads develop at the skin–stiffener interfaces which may lead to delamination and failure. Understanding the nature of these separation loads and being able to predict their magnitude accurately will enable the design of configurations with reduced tendencies for separation.

Several experimental and analytical investigations of the structural performance of composite stiffened panels under various loadings have been carried out. The following citations are meant only to serve as a summary and not as an exhaustive review. Stiffened panels under compression were studied by Knight and Starnes (1985) and Wiggenraad (1985). Panels under shear loading were investigated by Rouse (1987) while panels under pressure were treated by Hyer *et al.* (1990). In most investigations, the failure mode was found to be separation of the stiffeners from the skin in the postbuckling regime (Knight and Starnes, 1985; Rouse, 1987). The analytical studies made use of nonlinear finite elements to predict buckling and deflections and strains in the postbuckling regime (Knight and Starnes, 1985; Wiggenraad, 1985).

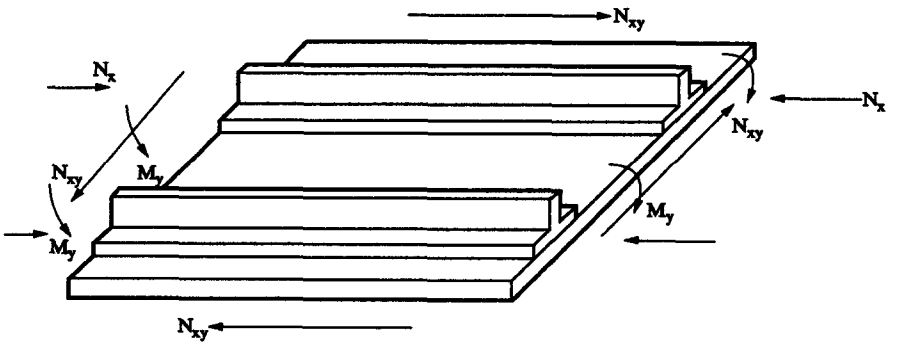

Fig. 1. Skin–stiffener combination (generalized loading).

The theoretical determination of the stresses at the skin–stiffener interface of composite stiffened structures has been relatively limited. Hyer and Cohen (1987) and Cohen and Hyer (1988) have performed a global–local analysis where the local solution in the flange-skin region is based on complex elasticity to calculate the stresses in stiffened panels under generalized loading and found that geometric nonlinearities can have a pronounced effect on the magnitude of the stresses at the skin–stiffener interface. Kassapoglou and DiNicola (1992) have solved the governing equations approximately, using energy minimization to obtain accurate interlaminar normal and shear stresses at the skin–stiffener interface for stiffened panels under compression and bending loads.

An approach analogous to that by Kassapoglou and DiNicola (1992) is proposed here to determine the interlaminar stresses at the skin–stiffener interface of composite stiffened panels under in-plane shear loads. It is more general since it treats the stress dependence on the longitudinal direction as an unknown function rather than a known function with unknown parameters.

The solution is based on the following assumptions: (1) The flange of the stiffener and the skin are each modeled as homogeneous orthotropic materials; (2) Stresses and strains do not depend on the transverse direction y (valid for configurations that are long in the y direction); (3) Away from the flange edge the in-plane stresses are at most linear in the out-of-plane direction z (not limiting; any power series or other Fourier expandable function can be assumed); (4) The final stress expressions are obtained by truncating the resulting infinite series after the first term (for higher accuracy more terms can be added).

The goal is to obtain simple and accurate expressions for stresses that can be used early in the design stage of a program to determine which candidate layups and materials are least prone to delamination without resorting to time consuming finite element or other solutions. In addition, with the stresses known accurately, delamination onset loads can be determined in conjunction with a three-dimensional stress-based failure criterion.

GOVERNING EQUATIONS AND SOLUTION APPROACH

The geometric configuration of the problem is shown in Fig. 2. The panel is assumed to be long in the transverse (y) direction so stresses and strains do not depend on that direction. The portion of the skin–stiffener combination that includes the edge of the flange and the skin directly below it, is isolated from the whole panel. The loads and boundary conditions at the ends of this local detail are assumed to be known (for example from a coarse finite element model).

The skin and flange are assumed to be homogeneous and orthotropic so that there is no coupling between loads and deformation (the **B** matrix and the A_{16}, A_{26}, D_{16} and D_{26} terms in the corresponding membrane and bending matrices are assumed to be zero). This assumption uncouples the governing equations and limits the applicability of the solution. The approach, however, can be generalized to any layup by suitably incorporating coupling terms in the energy expression. It is also assumed that there are two regions with smeared properties, the skin and the flange, each defined by nine elastic constants E_{11}, E_{22}, E_{33}, G_{12}, G_{13}, G_{23}, ν_{12}, ν_{13} and ν_{23}.

The case of in-plane tension (or compression) and bending moment was treated by Kassapoglou and DiNicola (1992). The governing equations were also derived in the reference by making use of the assumption that stresses and strains do not depend on the transverse direction y and by eliminating the out-of-plane stresses from the stress equilibrium, stress–strain and strain displacement equations. The final equations have the following (decoupled) form (Kassapoglou and DiNicola, 1992):

$$\frac{\partial^4 \sigma_{xx}}{\partial x^4} + \beta \frac{\partial^4 \sigma_{xx}}{\partial x^2 \partial z^2} + \gamma \frac{\partial^4 \sigma_{xx}}{\partial z^4} = 0, \tag{1}$$

$$\frac{\partial^2 \tau_{xy}}{\partial x^2} + \delta \frac{\partial^2 \tau_{xy}}{\partial z^2} = 0, \tag{2}$$

where

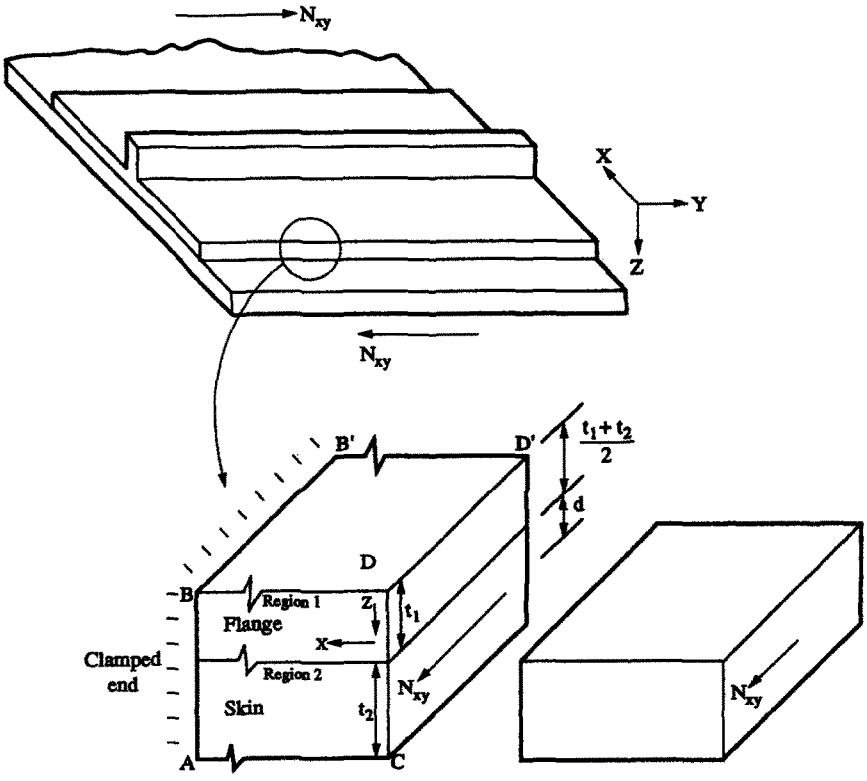

Fig. 2. Model for stiffener flange on skin (shear loading).

$$\beta = \frac{S_{55}S_{22} + 2S_{13}S_{22} - 2S_{12}S_{23}}{S_{22}S_{33} - S_{23}^2},$$

$$\gamma = \frac{S_{11}S_{22} - S_{12}^2}{S_{22}S_{33} - S_{23}^2},$$

$$\delta = \frac{S_{66}}{S_{44}},$$

and S_{ij}, $i\,j = 1, \ldots, 6$, are compliances of the region in which the equations are to be solved.

Under the assumptions stated above, for a pure shear load, σ_{xx} will be zero in the flange and the skin and only eqn (2) need be solved. A separation of variables solution can be developed for this equation by assuming the z dependence to be described by $\sin \lambda z$ and $\cos \mu z$, where λ and μ are chosen so as to satisfy stress-free boundary conditions at the top of the skin and the bottom of the flange. By selecting λ and μ to equal $n\pi/t_1$ in region 1 and $n\pi/t_2$ in region 2, and treating the x dependence as an unknown function, the following expressions are established for τ_{xy} in the flange (region 1) and the skin (region 2):

$$\tau_{xy} = \sum_{n=1}^{\infty} g_n(x)\left(C_3 \sin\frac{n\pi z}{t_1} + C_4 \cos\frac{n\pi z}{t_1}\right) + D_0 + D_1 z, \tag{3a}$$

$$\bar{\tau}_{xy} = \sum_{n=1}^{\infty} g_n(x)\left(\bar{C}_3 \sin\frac{n\pi z}{t_2} + \bar{C}_4 \cos\frac{n\pi z}{t_2}\right) + \bar{D}_0 + \bar{D}_1 z, \tag{3b}$$

where D_0, D_1, $\bar{D}_0$, $\bar{D}_1$ are known constants that describe the in-plane shear stress variation with z far from the flange edge. By assuming linear stress distribution, the effect of the twisting moment created by the applied shear load in Fig. 2 because of the moment arm d can be accounted for in the solution. The constants C_3, C_4, $\bar{C}_3$ and $\bar{C}_4$ are unknown at this

point. The functions $gn(x)$ should decay with large x so that the far field linear shear stress distribution can be recovered, i.e.

$$\lim_{x\to\infty}\tau_{xy} = D_0 + D_1 z,$$
$$\lim_{x\to\infty}\bar{\tau}_{xy} = \bar{D}_0 + \bar{D}_1 z. \tag{4}$$

Using the stress equilibrium equation:

$$\frac{\partial\tau_{xy}}{\partial x} + \frac{\partial\tau_{yz}}{\partial z} = 0, \tag{5}$$

and eqn (3a) the interlaminar shear stress τ_{yz} in region 1 is found to be

$$\tau_{yz} = -\sum_{n=1}^{\infty}\frac{\mathrm{d}g_n}{\mathrm{d}x}\left(-C_3\frac{t_1}{n\pi}\cos\frac{n\pi z}{t_1} + C_4\frac{t_1}{n\pi}\sin\frac{n\pi z}{t_1}\right) + H(x), \tag{6}$$

where $H(x)$ is an unknown function determined from the fact that at $z = 0$ (top of the flange), the shear stress τ_{yz} must be zero. This yields:

$$H(x) = \sum_{n=1}^{\infty}\frac{\mathrm{d}g_n}{\mathrm{d}x}\left(-C_3\frac{t_1}{n\pi}\right),$$

and the resulting expression for τ_{yz} is

$$\tau_{yz} = \sum_{n=1}^{\infty}\frac{\mathrm{d}g_n}{\mathrm{d}x}\left(C_3\frac{t_1}{n\pi}\left(\cos\frac{n\pi z}{t_1} - 1\right) - C_4\frac{t_1}{n\pi}\sin\frac{n\pi z}{t_1}\right). \tag{7a}$$

In an analogous way, using eqns (3b), (5), and the fact that $\bar{\tau}_{yz}$ must be zero at $z = t_2$ (bottom of the skin), the following expression is obtained for $\bar{\tau}_{yz}$ in region 2:

$$\bar{\tau}_{yz} = \sum_{n=1}^{\infty}\frac{\mathrm{d}g_n}{\mathrm{d}x}\left(\bar{C}_3\frac{t_2}{n\pi}\left(\cos\frac{n\pi z}{t_2} - \cos n\pi\right) - \bar{C}_4\frac{t_2}{n\pi}\sin\frac{n\pi z}{t_2}\right). \tag{7b}$$

Stress continuity at the interface between regions 1 and 2 implies that

$$\tau_{yz}(z = t_1) = \bar{\tau}_{yz}(z = 0). \tag{8}$$

Using eqns (7a) and (7b) to substitute in eqn (8), the following expression is obtained:

$$\sum_{n=1}^{\infty}\frac{\mathrm{d}g_n}{\mathrm{d}x}C_3\frac{t_1}{n\pi}(\cos n\pi - 1) = \sum_{n=1}^{\infty}\frac{\mathrm{d}g_n}{\mathrm{d}x}\bar{C}_3\frac{t_2}{n\pi}(1 - \cos n\pi). \tag{9}$$

If n is even, eqn (9) is identically satisfied. If n is odd, equating corresponding terms of the series in eqn (9) yields:

$$\bar{C}_3 = -C_3\frac{t_1}{t_2}. \tag{10}$$

To determine the functions $g_n(x)$, the complementary energy in regions 1 and 2 is minimized. The energy expression is

$$\Pi_c = \tfrac{1}{2}\int\int\int_V \boldsymbol{\sigma}^T \mathbf{S}\boldsymbol{\sigma}\,dV - \int\int_{A_\sigma} \mathbf{T}^T\bar{\mathbf{u}}\,dA_\sigma, \tag{11}$$

where the volume integral is taken over the whole volume of regions 1 and 2 and the surface integral is over the surface over which the tractions are given by the vector **T**, and the displacements $\bar{\mathbf{u}}$ are prescribed. In this case, the prescribed displacements are zero on the left surface ABB' of Fig. 2 and the ones on the right (CDD' on Fig. 2) will appear in terms that, after minimization, will not affect the functions $g_n(x)$. This was shown by Kassapoglou (1990). Thus, the second term of eqn (11) is neglected. Expanding the first term in eqn (11), the expression to be minimized has the form:

$$\Pi = \tfrac{1}{2}\int\int\int_V (S_{44}\tau_{yz}^2 + S_{66}\tau_{xy}^2)\,dx\,dy\,dz. \tag{12}$$

As an approximation, only the first term in the series is used. This was shown by Kassapoglou and DiNicola (1992) to be quite accurate for simple problems. Expression (12) can be evaluated per unit of y width since there is no dependence on y, and, after the z integrations have been carried out, the integral to be minimized becomes

$$\begin{aligned} I = \int_0^\infty \Bigg(& S_{44}\left(\frac{dg}{dx}\right)^2\left(\frac{3}{2\pi^2}C_3^2 t_1^3 + \frac{C_4^2 t_1^3}{2\pi^2} + \frac{4C_3C_4}{\pi^3}t_1^3\right) \\ & + S_{66}\left(g^2\left(C_3^2\frac{t_1}{2} + C_4^2\frac{t_1}{2}\right) + D_0^2 t_1 + D_1^2\frac{t_1^3}{3} + 2D_0D_1\frac{t_1^2}{2}\right. \\ & \left. + 2g\left(D_0C_3\frac{2t_1}{\pi} + D_1C_3\frac{t_1^2}{\pi} - D_1C_4\frac{2t_1^2}{\pi^2}\right)\right) + \bar{S}_{44}\left(\frac{dg}{dx}\right)^2\left(\frac{3}{2\pi^2}\bar{C}_3^2 t_2^3 + \frac{\bar{C}_4^2}{2\pi^2}t_2^3 - \frac{4\bar{C}_3\bar{C}_4}{\pi^3}t_2^3\right) \\ & + \bar{S}_{66}\left(g^2\left(\bar{C}_3^2\frac{t_2}{2} + \bar{C}_4^2\frac{t_2}{2}\right) + \bar{D}_0^2 t_2 + \bar{D}_1^2\frac{t_2^3}{3} + 2\bar{D}_0\bar{D}_1\frac{t_2^2}{2}\right. \\ & \left.\left. + 2g\left(\bar{D}_0\bar{C}_3\frac{2t_2}{\pi} + \bar{D}_1\bar{C}_3\frac{t_2^2}{\pi} - \bar{D}_1\bar{C}_4\frac{2t_2^2}{\pi^2}\right)\right)\right)dx. \end{aligned} \tag{13}$$

Minimization of I is done using calculus of variations which will give the governing differential equation for the unknown function g. The boundary conditions are also derived as conditions for g and its derivative at the flange edge and away from it ($x = \infty$). These are the same conditions as eqn (4) and the conditions that the flange edge be stress free. The Euler equation for g is then (Hildebrand, 1976):

$$\frac{d}{dx}\left(\frac{\partial I}{\partial g'}\right) - \frac{\partial I}{\partial g} = 0. \tag{14}$$

Using eqns (13) and (14) the resulting equation for g is

$$\begin{aligned} & \left(S_{44}t_1^3\left(\frac{3}{2\pi^2}C_3^2 + \frac{C_4^2}{2\pi^2} + \frac{4C_3C_4}{\pi^3}\right) + \bar{S}_{44}t_2^3\left(\frac{3}{2\pi^2}\bar{C}_3^2 + \frac{\bar{C}_4^2}{2\pi^2} - \frac{4\bar{C}_3\bar{C}_4}{\pi^3}\right)\right)\frac{d^2g}{dx^2} \\ & \qquad - \left(S_{66}t_1\left(\frac{C_3^2}{2} + \frac{C_4^2}{2}\right) + \bar{S}_{66}t_2\left(\frac{\bar{C}_3^2}{2} + \frac{\bar{C}_4^2}{2}\right)\right)g \\ & = S_{66}t_1\left(2\frac{D_0G_3}{\pi} + \frac{D_1C_3t_1}{\pi} - \frac{2D_1t_1C_4}{\pi^2}\right) + \bar{S}_{66}t_2\left(2\frac{\bar{D}_0\bar{C}_3}{\pi} + \frac{\bar{D}_1\bar{C}_3t_2}{\pi} - \frac{2\bar{D}_1t_2\bar{C}_4}{\pi^2}\right). \end{aligned} \tag{15}$$

The homogeneous solution is the required expression for g. The particular solution affects only the far field stress expression which is determined from the boundary conditions at large x [eqn (4)]. Thus, the solution for g is

$$g = K_1 e^{-\phi_3 x} + K_2 e^{+\phi_3 x}, \tag{16}$$

with ϕ_3 given by

$$\phi_3^2 = \frac{\pi^2}{t_1^2} \frac{S_{66} t_1 (C_3^2 + C_4^2) + \bar{S}_{66} t_2 (\bar{C}_3^2 + \bar{C}_4^2)}{S_{44} t_1 \left(3C_3^2 + C_4^2 + \frac{8C_3C_4}{\pi}\right) + \bar{S}_{44} \frac{t_2^3}{t_1^2} \left(3\bar{C}_3^2 + \bar{C}_4^2 - \frac{8\bar{C}_3\bar{C}_4}{\pi}\right)}. \tag{17}$$

To avoid ever increasing stresses with large x, the second term in eqn (16) is neglected. The stress expressions in regions 1 and 2 can now be determined using eqns (16), (3) and (7) as follows:

Region 1

$$\tau_{xy} = \sum_{n=1}^{\infty} e^{-\phi_3 x} \left(C_3 \sin \frac{n\pi z}{t_1} + C_4 \cos \frac{n\pi z}{t_1}\right) + D_0 + D_1 z,$$

$$\tau_{yz} = \sum_{n=1}^{\infty} \phi_3 e^{-\phi_3 x} \left(C_3 \frac{t_1}{n\pi} \left(1 - \cos \frac{n\pi z}{t_1}\right) + C_4 \frac{t_1}{n\pi} \sin \frac{n\pi z}{t_1}\right);$$

Region 2

$$\bar{\tau}_{xy} = \sum_{n=1}^{\infty} e^{-\phi_3 x} \left(\bar{C}_3 \sin \frac{n\pi z}{t_2} + \bar{C}_4 \cos \frac{n\pi z}{t_2}\right) + \bar{D}_0 + \bar{D}_1 z,$$

$$\bar{\tau}_{yz} = \sum_{n=1}^{\infty} \phi_3 e^{-\phi_3 x} \left(\bar{C}_3 \frac{t_2}{n\pi} \left(\cos n\pi - \cos \frac{n\pi z}{t_2}\right) + \bar{C}_4 \frac{t_2}{n\pi} \sin \frac{n\pi z}{t_2}\right). \tag{18}$$

It should be noted that, at this point, the constants C_3, C_4, $\bar{C}_3$ and $\bar{C}_4$ are unknown and, in general, will be functions of n as will be ϕ_3 which depends on these constants through eqn (17). To determine C_3 and C_4 the stress-free condition at $x = 0$ in region 1 is applied:

$$\sum_{n=1}^{\infty} \left(C_3 \sin \frac{n\pi z}{t_1} + C_4 \cos \frac{n\pi z}{t_1}\right) + D_0 + D_1 z = 0. \tag{19}$$

By expanding D_0 and $D_1 z$ in Fourier series, eqn (19) becomes:

$$\sum_{n=1}^{\infty} \left(C_3 \sin \frac{n\pi z}{t_1} + C_4 \cos \frac{n\pi z}{t_1}\right) + \sum_{n=1}^{\infty} \frac{2D_1 t_1}{n^2\pi^2} (\cos n\pi - 1) \cos \frac{n\pi z}{t_1}$$

$$+ \sum_{n=1}^{\infty} \frac{2}{n\pi} \left(D_0 + \frac{D_1 t_1}{2}\right) (1 - \cos n\pi) \sin \frac{n\pi z}{t_1} = 0, \tag{20}$$

and matching $\sin n\pi z/t_1$ and $\cos n\pi z/t_1$ terms:

$$C_3^{(2k-1)} = -\frac{4}{(2k-1)\pi} \left(D_0 + \frac{D_1 t_1}{2}\right),$$

$$C_4^{(2k-1)} = \frac{4D_1 t_1}{(2k-1)^2 \pi^2}, \tag{21}$$

where only odd terms in the series are included. Then, eqn (10) can be used to determine $\bar{C}_3$, and the only unknown left is $\bar{C}_4$.

To determine $\bar{C}_4$, the energy expression (11) is minimized. Again, the second term in that equation does not contribute. This is because the dependence on $\bar{C}_4$ of the second term in eqn (11) involves terms proportional to $\cos n\pi z/t_2$ which integrate to zero in the region $0 \leqslant z \leqslant t_2$. The expression (13) is used with g substituted from eqn (16). Carrying out the x integration, the part of the energy expression that depends on $\bar{C}_4$ becomes:

$$\bar{\Pi} = \frac{\bar{S}_{66}}{2}\left(\frac{1}{\phi_3}\left(\frac{4t_1^2}{t_2\pi^2}\left(D_0+\frac{D_1t_1}{2}\right)^2+\bar{C}_4^2\frac{t_2}{4}+16\frac{t_1}{\pi^2}\bar{D}_0\left(D_0+\frac{D_1t_1}{2}\right)\right.\right.$$
$$\left.\left.+8\bar{D}_1\frac{t_1t_2}{\pi^2}\left(D_0+\frac{D_1t_1}{2}\right)-4\frac{\bar{D}_1\bar{C}_4}{\pi^2}t_2^2\right)\right)$$
$$+\frac{\bar{S}_{44}}{2}\left(\phi_3\left(\frac{12t_1^2t_2}{\pi^4}\left(D_0+\frac{D_1t_1}{2}\right)^2+\frac{\bar{C}_4^2t_2^3}{4\pi^2}-\frac{8t_1t_2^2}{\pi^4}\bar{C}_4\left(D_0+\frac{D_1t_1}{2}\right)\right)\right). \quad (22)$$

Minimizing with respect to $\bar{C}_4$ amounts to differentiating eqn (22) with respect to $\bar{C}_4$ and setting the result equal to zero. This gives

$$\frac{\partial\bar{\Pi}}{\partial\bar{C}_4} = 0. \quad (23)$$

Solving for $\bar{C}_4$:

$$\bar{C}_4 = \frac{\phi_3^2\bar{S}_{44}\dfrac{8t_1t_2}{\pi^4}\left(D_0+\dfrac{D_1t_1}{2}\right)+\bar{S}_{66}4\dfrac{\bar{D}_1t_2}{\pi^2}}{\phi_3^2\bar{S}_{44}\dfrac{t_2^2}{2\pi^2}+\dfrac{\bar{S}_{66}}{2}}. \quad (24)$$

Equations (24) and (17) form a system of two equations in two unknowns, ϕ_3 and $\bar{C}_4$. Eliminating ϕ_3 gives the following cubic equation for $\bar{C}_4$:

$$T_3\bar{C}_4^3+T_2\bar{C}_4^2+T_1\bar{C}_4+T_0 = 0, \quad (25)$$

where the coefficients are given in the Appendix. Once eqn (25) is solved for $\bar{C}_4$ (using a Newton–Raphson algorithm in this investigation), ϕ_3 can be determined from eqn (24) rearranged as

$$\phi_3^2 = \frac{\bar{S}_{66}\left(\dfrac{4\bar{D}_1t_2}{\pi^2}-\dfrac{\bar{C}_4}{2}\right)}{\bar{S}_{44}\left(-\dfrac{8t_1t_2}{\pi^4}\left(D_0+\dfrac{D_1t_1}{2}\right)+\bar{C}_4\dfrac{t_2^2}{2\pi^2}\right)}. \quad (26)$$

It should be noted that only real and positive ϕ_3 values are accepted. This condition is used to select which of the three solutions for $\bar{C}_4$ in eqn (25) should be used. At this point the stress calculation is complete. The stresses are given by eqns (18) with C_3 and C_4 determined from eqn (21), $\bar{C}_3$ determined from eqn (10), $\bar{C}_4$ given by eqn (25), and ϕ_3 given by eqn (26). A simple FORTRAN computer code was written (SKINSTIF) implementing the solution.

SOLUTION VERIFICATION

As an example, the case shown in Fig. 3 was selected. The material properties are typical properties of graphite epoxy. It should be noted that due to the presence of the drop, the applied shear load creates a twisting moment that is reacted in the thick part of the structure (far from the flange edge) by shear stresses that vary linearly with thickness z (Timoshenko and Goodier, 1970). For the applied shear load of 2385.2 N (536 lb), resulting in a shear stress of 6.9 MPa (1000 psi), the constants in the far field shear stress distribution are given by:

$$D_0 = 6.9\,\text{MPa}\,(1000\,\text{psi}),$$
$$D_1 = -0.6\,\text{GPa m}^{-1}\,(-2221.9\,\text{psi in.}^{-1}),$$
$$\bar{D}_0 = 5.4\,\text{MPa}\,(777.8\,\text{psi}),$$
$$\bar{D}_1 = -0.6\,\text{GPa m}^{-1}\,(-2221.9\,\text{psi in.}^{-1}).$$

Using the far field stress distribution described by these quantities [eqn (4)] and the elastic constants shown in Fig. 3, the shear stresses τ_{xy} and τ_{yz} were calculated using the SKINSTIF software code mentioned in the previous section. The CPU time required for this run was negligible.

To check this solution, a finite element model was constructed using NASTRAN. The model comprised 8832 three-dimensional brick elements and 33,000 degrees of freedom. The finite element mesh is shown in Fig. 4. A typical run required over 11 minutes CPU time on an IBM 3090-600J. The results of the finite element solution for the τ_{xy} and τ_{yz} stresses at the flange–skin interface are compared to the present solution in Figs 5–7.

The in-plane shear stress τ_{xy}, normalized by the far field shear stress at that location is shown in Fig. 5. Both solutions show that, near the flange edge, the in-plane shear stress departs significantly from its far field value. The present solution goes to a finite value at the edge itself because only the first term in the series expression for τ_{xy} was used. For the complete series, the value at the edge itself would be zero since that is an imposed boundary

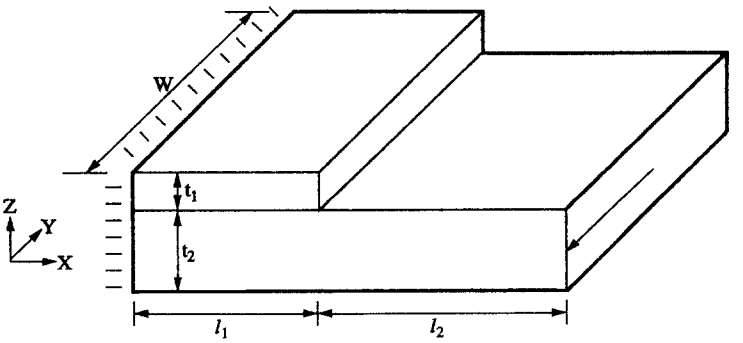

t_1 =0.00254m	(0.1 in)	E_x =130.2 GPa	(18.9 Msi)
t_2 =0.00508m	(0.2 in)	E_y =11.7 GPa	(1.7 Msi)
W=0.068m	(2.68 in)	E_z =11.7 GPa	(1.7 Msi)
l_1 =0.0381m	(1.5 in)	G_{xy}=5.0 GPa	(0.73 Msi)
l_2 =0.0381m	(1.5 in)	G_{xz}=5.0 GPa	(0.73 Msi)
		G_{yz}=3.9 GPa	(0.56 Msi)
		V_{xy}=0.29	
		V_{xz}=0.29	
		V_{yz}=0.5	

Fig. 3. Configuration for finite element model.

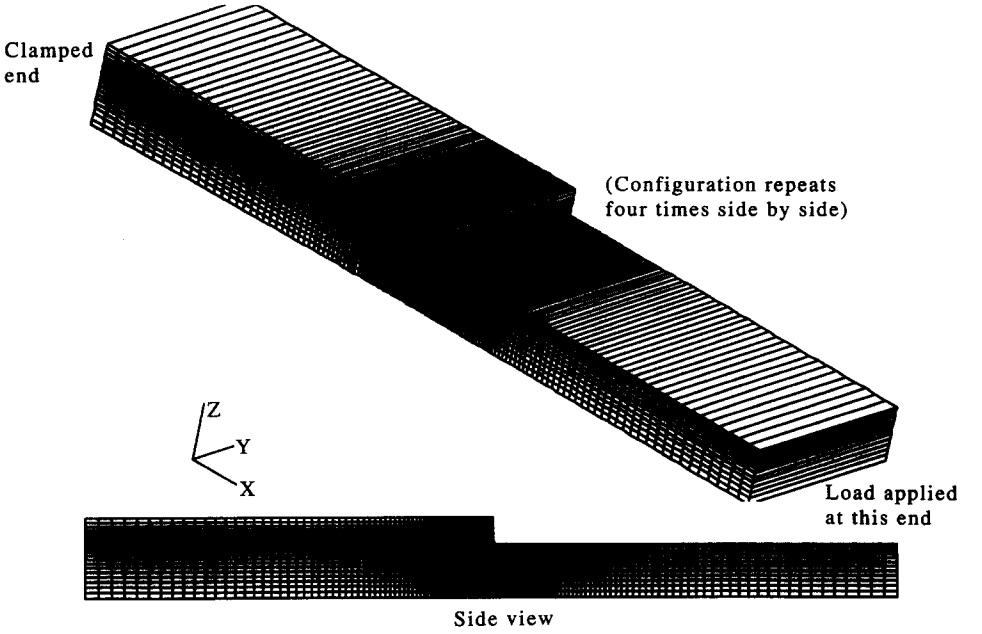

Fig. 4. Finite element mesh.

condition (flange edge is stress free). The finite element solution is, apparently, singular at the flange edge. Away from the edge it oscillates around the present solution departing significantly from it only very near the free edge. The finite element solution does not impose the stress-free boundary condition. This is an important difference since, for boundary layer problems with such steep stress gradients, not satisfying the stress-free boundary conditions can lead to very different results and singular stresses as Spilker and Chou (1980) have shown. Using hybrid elements and satisfying the traction-free-edge condition exactly, they showed that the stresses match closely those from displacement-based finite element solutions except at the edge itself where the latter solutions increase without bound while the hybrid element-based solutions are finite and recover the stress-free condition. For this reason, the discrepancy between the two solutions at the edge shown in Fig. 5 is not considered a drawback of the current approach. In any case, for improved accuracy, more terms in the series can be added. Less than one fifth of the flange thickness away from the

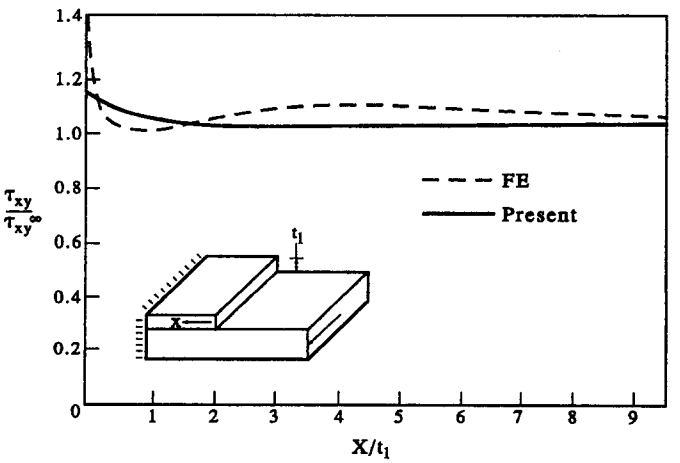

Fig. 5. In-plane shear stress τ_{xy} at flange–skin interface.

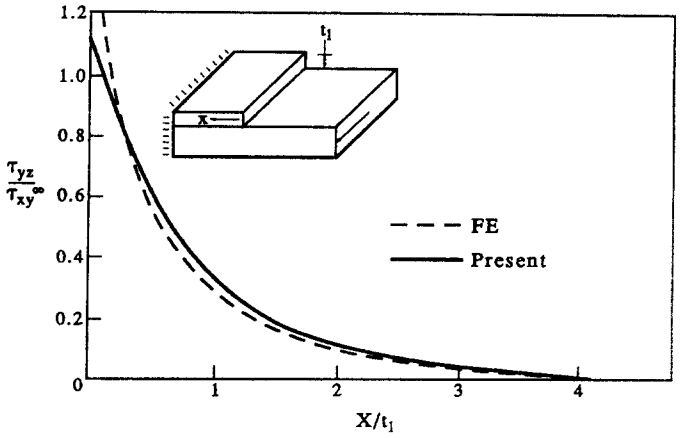

Fig. 6. Interlaminar shear stress τ_{yz} at flange–skin interface (flange thickness = 0.254 cm).

flange edge, the difference between the two solutions is less than 7% and becomes smaller with increasing distance from the free edge.

The interlaminar shear stress τ_{yz} normalized by the far field in-plane shear stress at the flange–skin interface is shown in Fig. 6. Excellent agreement between the two solutions is observed except right at the free edge where the finite element solution is, apparently, singular with the present solution being finite. This discrepancy is again due to the fact that only the first term in the series expression for the shear stresses was used. The complete series for τ_{yz} may be singular at the flange edge as was the case for the normal stress σ_{zz} [discussed by Kassapoglou and DiNicola (1992)] but the presence of $\bar{C}_4$ as an unknown in eqn (17) makes it hard to evaluate series convergence by inspection. It should be noted that at any other x value (larger than zero) the presence of the decaying exponential guarantees that the series for τ_{xy} and τ_{yz} are convergent.

To get an indication of the sensitivity of stresses on flange thickness, the same problem was solved with the flange reduced to 40% of its previous thickness. The interlaminar shear stress τ_{yz} is shown in Fig. 7. Again, excellent agreement is found between the present solution and the finite element results except right at the flange edge. Figure 7 shows that, reducing the flange thickness reduces the interlaminar shear stress as should be expected since in the limiting case of zero flange thickness the interlaminar shear stress would be identically zero.

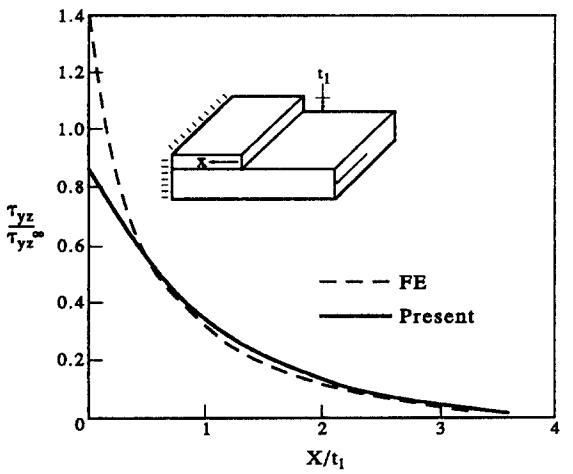

Fig. 7. Interlaminar shear stress τ_{yz} at flange–skin interface (flange thickness = 0.106 cm).

Comparison of the in-plane shear stress τ_{xy} for this case gives results very similar to Fig. 5. The results in Figs 6 and 7 suggest that the method is accurate and reliable.

CONCLUSIONS

A simple closed form solution has been developed for determining the stresses at the flange–skin interface of orthotropic materials under shear loads. The present solution was found to be in very good agreeement with finite element solutions even if only the first term in the series expression is used. This solution is very efficient since it is in closed form and makes it possible to obtain accurate stress solutions at flange–skin interfaces. These can then be used in preliminary design in conjunction with a stress failure criterion to predict onset of delamination or can be used to compare with stresses from other layup, material and geometry configurations to select the least delamination prone candidate.

REFERENCES

Cohen, D. and Hyer, M. W. (1988). Influence of geometric nonlinearities on skin–stiffener interface stresses. AIAA Paper 88-2217, presented at the 29th SDM Conference, Williamsburg, VA, April 1988.

Hildebrand, F. B. (1976). *Advanced Calculus for Applications*. Prentice-Hall, Englewood Cliffs, NJ.

Hyer, M. W. and Cohen, D. (1987). Calculation of stresses and forces between the skin and stiffener in composite panels. AIAA Paper 87-0731, presented at the 28th SDM Conference, Monterey, CA, April 1987.

Hyer, M. W., Loup, D. C. and Starnes, J. H. (1990). Stiffener/skin interactions in pressure loaded composite panels. *AIAA Jl* **28,** 532–537.

Kassapoglou, C. (1990). Determination of interlaminar stresses in composite laminates under combined loads. *J. Reinforced Plastics and Composites* **9,** 33–58.

Kassapoglou, C. and DiNicola, A. J. (1992). Efficient stress solutions at skin–stiffener interfaces of composite stiffened panels. *AIAA Jl* **30,** 1833–1839.

Knight, N. F. and Starnes, J. H. (1985). Postbuckling behavior of selected curved stiffened graphite–epoxy panels loaded in compression. AIAA Paper 85-0768.

Rouse, M. (1987). Postbuckling and failure characteristics of stiffened graphite–epoxy shear webs. AIAA Paper 87-0733, presented at the 28th SDM Conference, Monterey, CA, April 1987.

Spilker, R. L. and Chou, S. C. (1980). Edge effects in symmetric composite laminates: Importance of satisfying the traction-free edge condition. *J. Composite Materials* **14,** 2–20.

Timoshenko, S. P. and Goodier, J. N. (1970). *Theory of Elasticity*. McGraw-Hill, New York.

Wiggenraad, J. F. M. (1985). Postbuckling behavior of blade stiffened carbon–epoxy panels loaded in compression. NLR MP85019, Amsterdam, February 1985.

APPENDIX

The coefficients in the equation for $\bar{C}_4$ [eqn (25)] are as follows:

$$T_3 = -\bar{S}_{44}\bar{S}_{66}t_2^3,$$

$$T_2 = 4\bar{S}_{66}\bar{S}_{44}\frac{t_2^2}{\pi}\left(t_2\bar{C}_3+\frac{t_2}{\pi}\bar{D}_1t_2+\frac{2t_1}{\pi}\left(D_0+\frac{D_1t_1}{2}\right)\right),$$

$$T_1 = -\bar{S}_{44}\bar{S}_{66}t_2^3\bar{C}_3\left(2\bar{C}_3+32\frac{\bar{D}_1t_2}{\pi^3}\right)-S_{44}\bar{S}_{66}\frac{t_1^3}{2}\left(3C_3^2+C_4^2+\frac{8C_3C_4}{\pi}\right)-\bar{S}_{44}S_{66}\frac{t_1t_2^2}{2}(C_3^2+C_4^2),$$

$$T_0 = S_{44}\bar{S}_{66}\frac{4t_1^3}{\pi^2}\bar{D}_1t_2\left(3C_3^2+C_4^2+\frac{8C_3C_4}{\pi}\right)+\bar{S}_{44}S_{66}\frac{8t_1^2t_2}{\pi^2}\left(D_0+\frac{D_1t_1}{2}\right)(C_3^2+C_4^2)$$
$$+\bar{S}_{44}\bar{S}_{66}\frac{4t_2^2}{\pi^2}\bar{C}_3^2\left(3t_2\bar{D}_1t_2+2t_1\left(D_0+\frac{D_1t_1}{2}\right)\right).$$